

# NANODIAMOND SYNTHESIS AND CHARACTERIZATION, AS WELL AS ITS USE AS AN ANTI-POLISHING AGENT ON SiO<sub>2</sub> SUBSTRATE

Durlab Das<sup>a</sup>, S. Venkatesan<sup>b</sup>, KARTHIK A., Assistant Professor, Department of Aeronautical Engineering, Dhanalakshmi Srinivasan College of Engineering & Technology, Chennai, India. Assistant Professor, Department of Mechanical Engineering, Dhanalakshmi Srinivasan College of Engineering and Technology, India, [durlav1993@gmail.com](mailto:durlav1993@gmail.com)<sup>b</sup>, [venkatesans.mech@dscet.ac.in](mailto:venkatesans.mech@dscet.ac.in), [karthik a@gmail.com](mailto:karthik_a@gmail.com)

## ABSTRACT:

Nanodiamond particles were produced, purified, and described in the current work. The surface of the nanodiamond was then oxidised to create a uniform coating of COOH groups. Finally, the functionalized particles were placed on the SiO<sub>2</sub> substrate and their anti-polishing properties were studied. FT-TR, TGA, TEM, and SEM were used to characterise the products of this study

Keywords: Nanodiamond; Surface modification; SiO<sub>2</sub>-based substrate

## INTRODUCTION:

Diamond has a highly compact structure and is an excellent insulator. Any contaminants can cause large changes in electron levels [1-3]. One of the most notable characteristics of diamond is its high heat conductivity, which is about five times that of copper [4]. Diamonds also have a high Young's modulus, a high tensile stress, a low friction coefficient, and a melting temperature of around 4000°C. Diamond also has a high chemical stability, since it is resistant to most acids and alkalis. Diamond naturally is formed under high pressures during along time. Nano-sized diamond can be prepared through detonation of an explosive deficient in oxygen such that the oxygen cannot oxidize all of the other elements (C, H and N) in the explosive. When such an explosive is detonated, the released free carbon atoms can coagulate and rearrange under the high-temperature and high-pressure condition produced by the detonation reaction, to form Nano-sized diamond crystallites. In the mid-1980s, Nano-sized diamond was found in the detonation residue of some high-energy explosives after they were exploded in an inert gas environment. Adjustable surface textures, and a tiny and narrow size distribution have made nano-sized diamond particles well-known. These nanoparticles exhibit unusual mechanical, electrical, and optical properties and thermal characteristics. It's worth noting that nano-sized diamond particles can be stabilised by adding functional groups to the surface to prevent further agglomeration.

The goal of this research is to first functionalize nano-sized diamonds to prevent agglomeration before depositing them on the surface of SiO<sub>2</sub> lenses. SiO<sub>2</sub> is a chemically inert substrate that does not react. The optical qualities of the SiO<sub>2</sub> substrate should be preserved after covering it with Nano-sized diamond. Nano-sized diamond coating on SiO<sub>2</sub> substrate induces features such as Nano-sized diamond hardness, high-temperature endurance without affecting the lens' optical properties, high-pressure tolerance, and so on. This method's end product might be used in camera hatches and windows of devices that can withstand high temperatures and pressures. Nano-sized diamond particles were created in this

case, and the surface of the nano-sized diamond particles was oxidised by a mineral combination.

### **Materials and physical measurements:**

All chemicals and solvents were acquired commercially and utilised without any additional purification. A HITACHI S-4160 operating at 30 kV was used for scanning electron microscopy (SEM). The WQF-510A FTIR spectrometer was used to capture FT-IR spectra. A Mettler thermogravimetric analyzer was used to perform thermogravimetric analysis (TGA) in the temperature range of ambient to 800°C in air atmospheres at a heating rate of 10°C/min. Images were taken using a Philips EM 280 transmission electron microscope with a 150 kV accelerating voltage. By using the explosion technique, nano-sized diamond particles were produced from a 50/50 combination of TNT and RDX [14]. The as-prepared particles contained impurities such as metals and carbons, which were eliminated using purification procedures such as chemical and thermal treatments, as detailed in the following sections.

### **Purification process of synthesized ND:**

A suitable amount of raw material was combined with 90 ml of 37 percent HCl and heated to 100°C for 1 hour under guidance. Then, to eliminate any remaining contaminants, a solution of potassium permanganate and H<sub>2</sub>SO<sub>4</sub> was added and agitated overnight. The particles were then filtered, rinsed, and dispersed in 200 mL of 1:1 HCl/HNO<sub>3</sub> solution. To eliminate any metal impurities, this mixture was heated and boiled for 2 hours. Thermal oxidation at 400°C for 5 hours eliminated the carbon impurities contained the carbon-like phase.

### **Oxidation of ND surface:**

With minor modifications, ND-COOH was produced according to the literature [15]. In a typical technique, 5.0 g of Nano-sized diamond particles were sonicated in a water bath for 30 minutes with 120 ml of H<sub>2</sub>SO<sub>4</sub> (98%) and HNO<sub>3</sub> (68%) (V:V=3:1). The resultant mixture was agitated for 7 days at 80°C. After that, the reaction solution was centrifuged and the solid residue was thoroughly rinsed with water. To get the dry powder of ND-COOH, the samples were dried under vacuum at 60°C overnight.

### **Chemical chlorination of nanodiamond:**

At 70°C for 24 hours, 0.1 g of ND-COOH was refluxed in 30 ml of toluene containing 10 ml of thionyl chloride (SOCl<sub>2</sub>) to convert carboxyl groups to acyl chloride groups. Finally, leftover SOCl<sub>2</sub> was evaporated under vacuum using a rotary evaporator, and the samples were collected.

### **Preparation of stable ND-Cl suspension solution:**

To disperse the ND-Cl in the solvent, 10 mg of ND-Cl was combined with 40 ml of o-dichlorobenzene and sonicated in a water bath for 2 hours. It was then left to settle for four days in order to achieve a steady suspension. The top 20 mL solution was then decanted for further use.

### **Preparation of aminated SiO<sub>2</sub>-based substrate:**

The glass substrate was initially immersed for 1 hour in a piranha solution (7:3 v/v H<sub>2</sub>SO<sub>4</sub>/H<sub>2</sub>O<sub>2</sub>) at 80°C. It was then cleaned with water and dried with a N<sub>2</sub> gas stream. On a rotating plate, the cleaned glass substrate was submerged in a 2 percent APTES ethanol solution for 30 minutes. It was then washed

with ethanol. After that, the substrate was cured overnight at 50°C.

### Fabrication of ND-coated SiO<sub>2</sub>-based substrate:

The APTES-treated glass substrate was placed in a glass bottle with a capacity of 50 mL. The container covering the substrate was then filled with 20 mL stable ND-Cl suspension and a few drops of pyridine. The bottle was placed in a 140°C oven for 24 hours. The resultant substrate was washed with ethanol once the reaction was done.

### Results and Discussion:

The nanodiamond samples' X-ray diffraction (XRD) patterns are shown in FIG. 1, demonstrating that the crystallites formed have a cubic structure. The samples' graphitization has also been accepted. (002) graphite planes have a large diffraction peak at  $2\theta=25^\circ$ . (FIG. 1a). After thermal treatment, this peak vanished, however the intensity of (111) diamond planes at  $2\theta=43.5^\circ$  rose (FIG. 1b). The broadened peaks further demonstrate the items' tiny size.

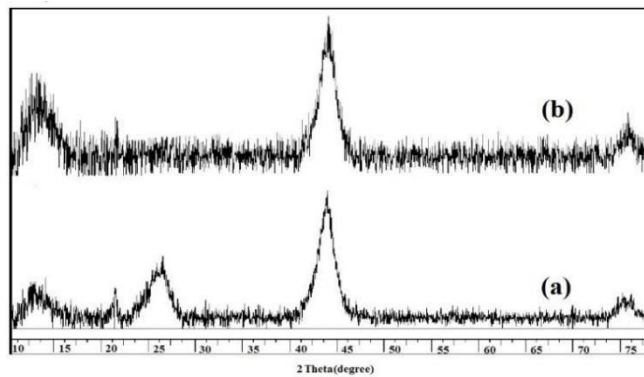


FIG.1.XRD pattern of the synthesized samples before (a) and after (b) annealing process.

### Surface modification:

FIG. 2 shows the IR spectra of nano-sized diamond particles before surface treatment. Functional groups such as C–H (2783 cm<sup>-1</sup> and 2858 cm<sup>-1</sup> stretching and 1321 cm<sup>-1</sup> bending) and O–H vibrations were clearly seen in the pure Nano-sized diamond (3300-3500 cm<sup>-1</sup> stretching). Furthermore, the presence of C–O and C–O–C ether vibrations is demonstrated by a broad weak signal in the 1012-1165 cm<sup>-1</sup> range [16].

FIG. 3 presents the thermal degradation behavior of Nano-sized diamond particles. Results show that the TGA curve of pristine Nano-sized diamond particles can be divided to four temperature regions. In the first region “I” (30°C-220°C), an initial decrease (~3 wt %) in weight is observed due to desorption of adsorbed water. In the second region “II” (220°C-400°C), the weight of the sample is approximately constant. It is interesting to note that an increase in the weight of Nano-sized diamond particles is observed in the third region “III” (400°C-520°C) with a maximum around 500°C due to the oxidation of “light” C–H bonds to “heavier” C=O or C–O bonds. The thermal degradation behaviour of Nano-sized diamond particles is shown in Figure 3. The TGA curve of pure Nano-sized diamond particles may be separated into four temperature areas, according to the findings. Due to the desorption of adsorbed water, the first zone "I" (30°C-220°C) shows an initial drop in weight

(3%). The weight of the sample is nearly constant in the second zone "II" (220°C-400°C). It's worth noting that the oxidation of "light" CH bonds to "heavier" C=O or CO bonds causes a rise in the weight of Nano-sized diamond particles in the third area "III" (400°C-520°C), with a maximum around 500°C. A large decline in the fourth area (>520°C) "IV" The etching of diamond by oxidation in air causes a considerable drop in the weight of Nano-sized diamond particles in the fourth area (>520°C) "IV" [17]. The temperature at which diamond phase breakdown begins is 550°C. At 800°C, the ND sample had a residual mass of roughly 60%, indicating that the Nano diamond material had excellent thermal stability.

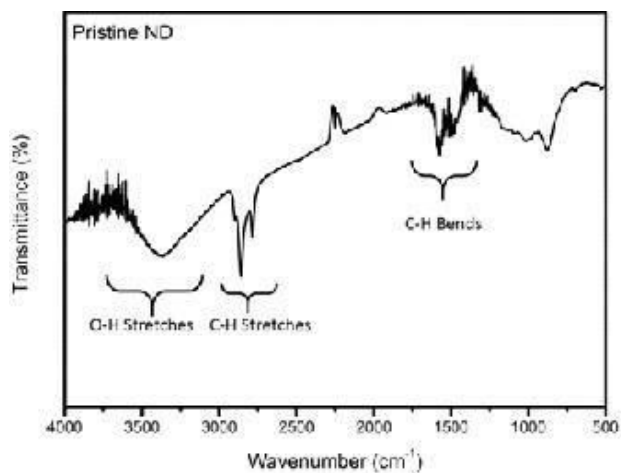


FIG.2. IR spectrum of pristine ND particles.

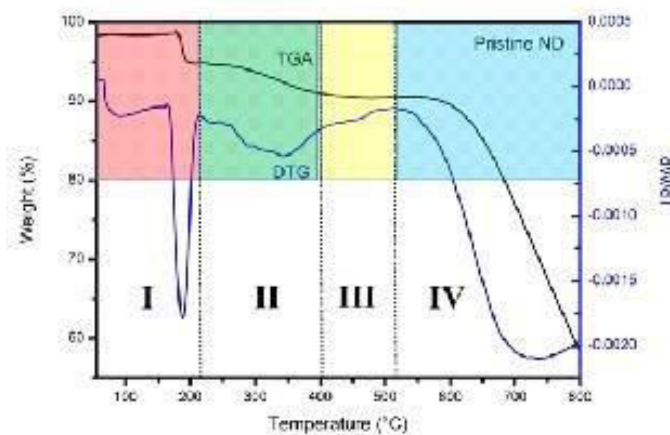


FIG.3. TGA/DTG curves of the pristine ND particles.

**Carboxylated ND particles (ND-COOH):**

FIG. 4 shows the FT-IR spectra of ND-COOH particles following surface oxidation. FT-IR spectra of ND-COOH particles reveals a significant peak centred at 1720 cm<sup>-1</sup>, which is due to the carbonyl group (C=O), in contrast to pure Nano-sized diamond particles. In addition, the OH stretching vibrations are linked to the weaker band in the 3000-3700 cm<sup>-1</sup> range [18,19].

FIG.4. IR spectrum of ND-COOH particles.

TGA was used to assess the thermal stability of the ND-COOH sample (FIG. 5). It should be noted that when heated from ambient temperature to 180°C, the ND-COOH sample loses roughly 3% more water than the pure ND sample. Because of the presence of C=O groups on the surface of ND-COOH, it is somewhat more hydrophilic than virgin ND. In addition, between 200°C and 550°C, the weight of ND-

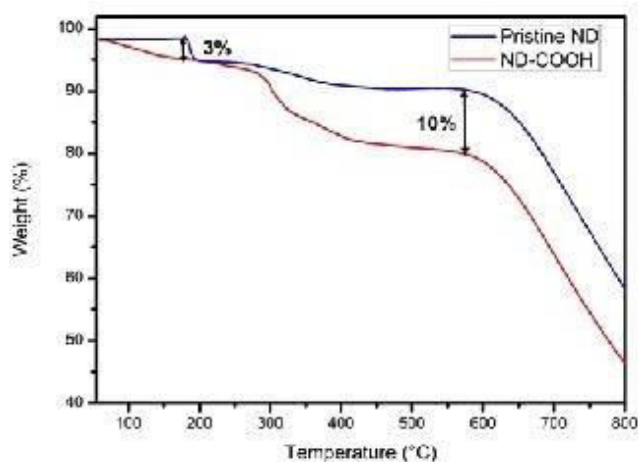


FIG.5. Thermogravimetric curves of the pristine ND particles and ND-COOH.

### Chlorinated ND particles (ND-Cl):

FT-IR analysis revealed the first sign of effective surface chlorination using thionyl chloride (FIG. 6). The existence of C-Cl group stretching vibration can be attributed to a strong intensity peak at 790 cm<sup>-1</sup> [22]. It's worth noticing that the C=O and O-H vibrations are absent from this spectrum, showing that chlorination is complete.

TGA was used to investigate the thermal stability of the ND-Cl material (FIG. 7). It should be observed that when heated from room temperature to 200°C, the ND-Cl sample loses around 4% less water than the ND-COOH sample. Because of the presence of C-Cl groups on the surface of ND-Cl, it is less hydrophilic than ND-COOH. The size of the Nano-sized diamond before and after functionalization was investigated using TEM imaging. TEM pictures of pure Nano-sized diamond particles (FIG. 8a) and ND-COOH particles (FIG. 8b) were acquired in this respect, and it was established that the reaction condition had no substantial influence on particle size and agglomeration. FIG.6. IR spectrum of ND-Cl particle

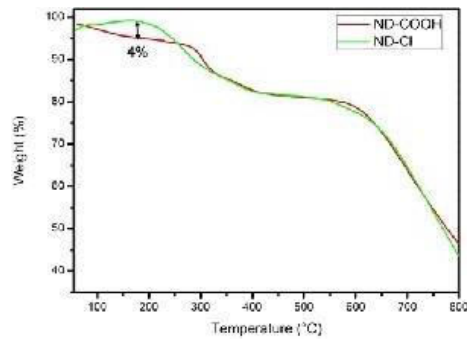


FIG.7. Thermogravimetric curves of the ND-Cl and ND-COOH particles.

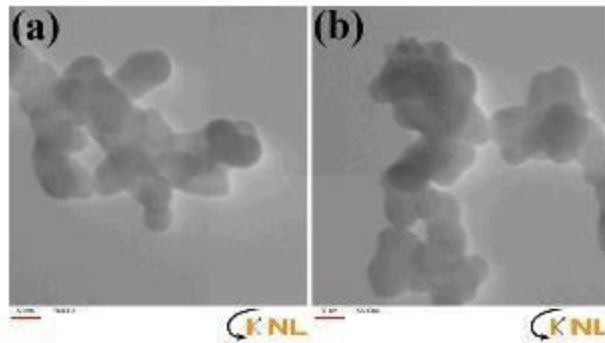


FIG.8. TEM images of the pristine ND particles (a) and ND-COOH particles (b).

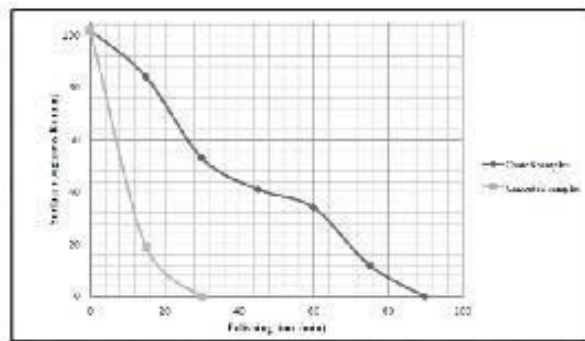
### ND-coated SiO<sub>2</sub>-based substrate:

The glass substrate was effectively coated with nano-sized diamond particles, as evidenced by SEM images. No particles are visible on the surface of the glass substrate before change, as shown in FIGS. 9a, b. On the other hand, FIG. 9c clearly demonstrates that Nano-sized diamond particles were efficiently deposited on the glass substrate's surface. A high-magnification SEM image indicated that the ND-coated substrate is less than 100 nm thick (FIG.

9d). FIG.9. SEM images of glass substrates before modification (a and b) and after coating with ND particles (c and d) at different magnifications.

The polishing trials were carried out using a laboratory-scale system that had two rotational shafts operated by separate electric motors and a container filled with abrasive materials. The substrate for spindle B was placed at the bottom of the container. The abrasive grinding wheels and polishing pads were mounted on spindle A, which was subjected to a polishing load of 1.5 N. The surface roughness of the substrate was examined as a function of polishing time before and after treatment with Nano-sized diamond. Surface coating with Nano-sized diamond improves roughness in contrast to untreated samples, as shown in FIG. 10.

FIG.10. Surface roughness of the substrate.



## CONCLUSION:

The contaminants like as metals and carbon were eliminated by acidizing and thermal oxidation, respectively, after the ND particles were produced by explosion. Chemical techniques were used to encapsulate purified materials on glass substrates. The substrate was subsequently examined, and it was discovered that a nano-sized diamond covering enhanced the roughness of the substrate.

Acknowledgment

## REFERENCES:

1. Maier F, Riedel M, Mantel B, et al. Origin of surface conductivity in diamond. *Physical Review Letters*. 2000; 85(16):3472.
2. Gu E, Choi HW, Liu C, et al. Reflection/transmission confocal microscopy characterization of single-crystal diamond microlens arrays. *Applied Physics Letters*. 2004; 84(15):2754-6.
3. Savvides N. Optical constants and associated functions of metastable diamond-like amorphous carbon films in the energy range 0.5-7.3 eV. *J App Phy*. 1986; 59(12):4133-45.
4. Graebner JE, Jin S, Kammlott GW, et al. Large anisotropic thermal conductivity in synthetic diamond films. *Nature*. 1992; 359(6394):401.
5. Kaner RB, Gilman JJ, Tolbert SH. Designing superhard materials. *Science*. 2005; 308(5726):1268-9
6. Troupe CE, Drummond IC, Graham C, et al. Diamond-based glucose sensors. *Diamond and Related Materials*. 1998; 7(2-5):575-80.
7. Korobeinichev OP, Ermolin NE, Chernov AA, et al. Flame structure, kinetics and mechanism of chemical reactions in flames of mixed composition based on ammonium perchlorate and polybutadiene rubber. *Combustion, Explosion and Shock Waves*. 1992; 28(4):366-71.
8. Greiner NR, Phillips DS, Johnson JD, et al. Diamonds in detonation soot. *Nature*. 1988; 333(6172):440-5.
9. Schrand AM, Hens SA, Shenderova OA. Nanodiamond particles: Properties and perspectives for bioapplications. *Critical Reviews in Solid State and Materials Sciences*. 2009; 34(1-2):18-74.
10. Mochalin VN, Shenderova O, Ho D, et al. The properties and applications of nanodiamonds. *Nature Nanotechnology*. 2012; 7:11-23.

11. Shenderova OA, McGuire GE. Science and engineering of nanodiamond particle surfaces for biological applications. *Biointerphases*. 2015;10(3):030802.
12. Nagl A, Hemelaar SR, Schirhagl R. Improving surface and defect center chemistry of fluorescent nanodiamonds for imaging purposes—a review. *Analytical and Bioanalytical Chemistry*. 2015;407(25):7521-36.
13. Jabeen S, Kausar A, Muhammad B, et al. A review on polymeric nanocomposites of nanodiamond, carbon nanotube and nanofiller: Structure, preparation and properties. *Polymer-Plastics Technology and Engineering*. 2015;54(13):1379-409.
14. Efremov VP, Zakatilova EI. The analysis of thermal stability of detonation nanodiamond. *J Phys: Conference Series*. 2016;774(1):012014.
15. Cheng J, He J, Li C, et al. Facile approach to functionalize nanodiamond particles with V-shaped polymer brushes. *Chemistry of Materials*. 2008;20(13):4224-30.
16. Wang Z, Xu C, Liu C. Surface modification and intrinsic green fluorescence emission of a detonation nanodiamond. *Journal of Materials Chemistry C*. 2013;1(40):6630-6.
17. Stehlik S, Varga M, Ledinsky M, et al. Size and Purity Control of HPHT Nanodiamonds down to 1 nm. *The Journal of Physical Chemistry C*. 2015;119(49):27708-20.
18. Kozak H, Remes Z, Houdkova J, et al. Chemical modifications and stability of diamond nanoparticles resolved by infrared spectroscopy and Kelvin force microscopy. *J Nanoparticle Res*. 2013;15:1568-72.
19. Chung PH, Perevedentseva E, Tu JS, et al. Spectroscopic study of bio-functionalized nanodiamonds. *Diamond and Related Materials*. 2006;15(4-8):622-5.
20. Wahab Z, Foley EA, Pellechia PJ, et al. Surface functionalization of nanodiamond with phenylphosphonate. *Journal of Colloid and Interface Science*. 2015;450:301-9.
21. Bousa D, Luxa J, Mazanek V, et al. Toward graphene chloride: Chlorination of graphene and graphene oxide. *RSC Advances*. 2016;6(71):66884-92.
22. Lisichkin GV, Korol'kov VV, Tarasevich BN, et al. Photochemical chlorination of nanodiamond and interaction of its modified surface with C-nucleophiles. *Russian Chemical Bulletin*. 2006;55(12):2212



